Supporting information

CO_2 and CH_4 Separation by Adsorption Using Cu-BTC Metal-Organic Framework

Lomig Hamon, Elsa Jolimaître, and Gerhard D. Pirngruber[*]

IFP-Lyon, Catalysis and Separation Division, Rond-point de l'échangeur de Solaize, 69360 Solaize, France.

Corresponding author. E-mail: gerhard.pirngruber@ifp.fr

RECEIVED DATE (to be automatically inserted after your manuscript is accepted if required according to the journal that you are submitting your paper to)

CO_2 and CH_4 Separation Using Cu-BTC MOF

Tel. +33 478 022 733, fax. +33 478 022 066.

Experimental details of the breakthrough curve measurements

Figure S1 shows a scheme of the setup used for the breakthrough experiments at high pressure. Different gas mixtures can be prepared by a set of mass flow controllers. The gas mixture is either sent to the adsorption column, which is placed in an oven, or to a bypass line. A backpressure regulator is placed downstream of the column and fixes the pressure in the column and by-pass line. Downstream of the backpressure regulator, the column effluent is diluted with helium and is then analyzed by a mass

spectrometer. The dilution is necessary since the response of the mass spectrometer is linear only in a concentration range of 0–15%. The dilution brings the concentrations of the eluted gases down to this range. Moreover, it keeps the total flow rate more or less constant, which is a necessary condition for obtaining correct mass balances. Mass 44 is used for analysis of CO_2, mass 15 for the analysis of CH_4 (mass 16 is avoided because CO_2 contributes to the intensity) and mass 28 for the analysis of CO (after subtraction of the contribution of CO_2). The signals are normalized by the intensity of mass 4 (He), in order to correct for drifts in the mass spectrometer.

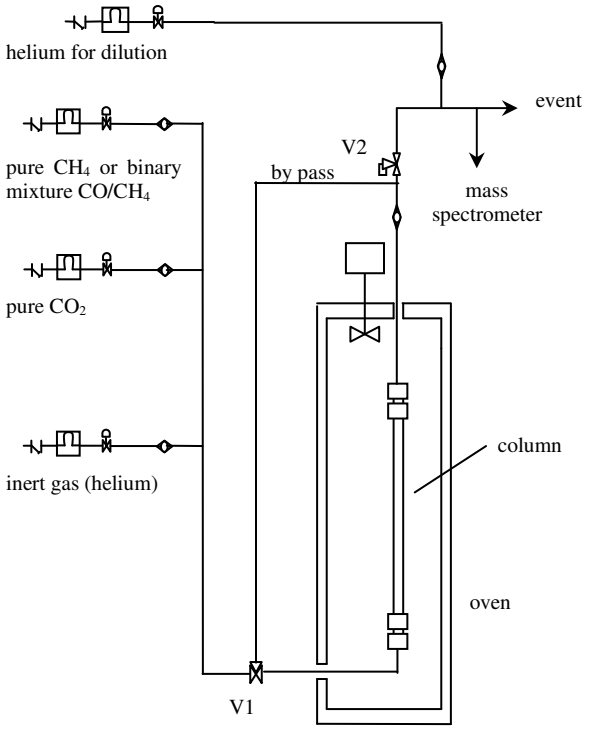

Figure S1. Scheme of the setup used for breakthrough experiments.

In practice, the experiment is conducted as follows: The column is filled with adsorbent (here in the form of powder) and placed in the oven. The adsorbent is activated in flow of 1.0 $NL{\cdot}h^{-1}$ of helium at a temperature of 473 K. After keeping that temperature for the desired amount of time, the oven is brought back to the temperature of the breakthrough experiment. The pressure is raised to the desired level and the flow of helium used for the downstream dilution is switched on (200 $NL{\cdot}h^{-1}$). The column is then isolated by turning the two valves up-stream and down-stream of the column (as shown in the in

Figure), *i.e.* it remains filled with helium at the pressure of the experiment. The gas mixture to be used for the breakthrough experiments is then prepared. Total flow is fixed at 4.0 $nL \cdot h^{-1}$ for all adsorption experiments. It flows *via* the by-pass line to the mass spectrometer. Once the mass spectrometer signals of the feed mixture have been stabilised the breakthrough experiment is started by turning the valves V1 and V2.

The raw breakthrough curves therefore have the following appearance: At the beginning, *i.e.* before turning valve V1, the mass spectrometer detects the feed mixture. Once the feed is directed to the column by turning valve V1 it pushes the helium that was left in the column. The concentration of the other components decreases and only helium is detected in the mass spectrometer until breakthrough of the first component occurs. It is important to take into account the dead time when determining breakthrough time: this dead time corresponds to the gas crossing from V1 to the column and from the outlet of the column to the mass spectrometer. The knowledge of these volumes allows a determination of the dead time as a function of flow.

In order to fully regenerate the column for the next procedure the initial activation procedure is repeated between each breakthrough experiment. The mass of the dry adsorbent is determined at the end of a series of experiments.

In the Figures, breakthrough curves are represented in the form of the normalized flow rates $F_i/F_{i,0}$, F_i being the measured flow rate of component i at the column outlet and $F_{i,0}$ being the feed flow rate of component i.

Characterization results

The XRD pattern of sample is similar to the theoretical one (see Figure S2). To check the thermal stability of the Cu-BTC, TGA measurements were performed (see Figure S3). A weight loss up to 350 K could correspond to the removal of free trimesic acid, ethanol and free water coming from the synthesis. Between 350 K and 460 K, a second weight loss corresponds to the dehydration of the water

molecules which were linked to the copper: this loss of 29% of weight corresponds to the transition from the $Cu_3(BTC)_2(H_2O)_3$ form to the non-hydrated $Cu_3(BTC)_2$ form. Above 550 K, the material is destroyed. This TGA measurement suggests that the best outgassing temperature under helium atmosphere is around 470 K. To check the regenerability of this material, a cycled TG was recorded between 298 K and 473 K (Figure S4). For the first cycle, the TG curve presented the same shape as previously observed. During the next cycles, the weight remained constant proving the good choice of the activation and outgassing temperature.

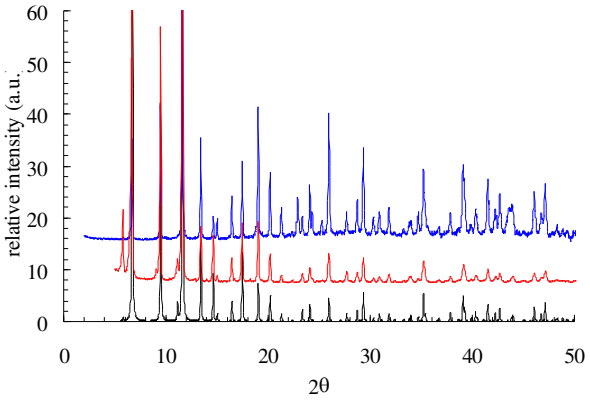

Figure S2. Calculated XRD pattern (black), XRD of a commercial Cu-BTC (red) and of the the Cu-BTC used in this study (blue).

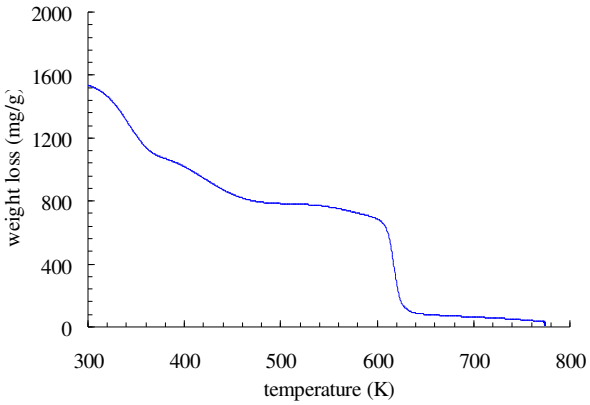

Figure S3. Thermogravimetric analysis of the Cu-BTC.

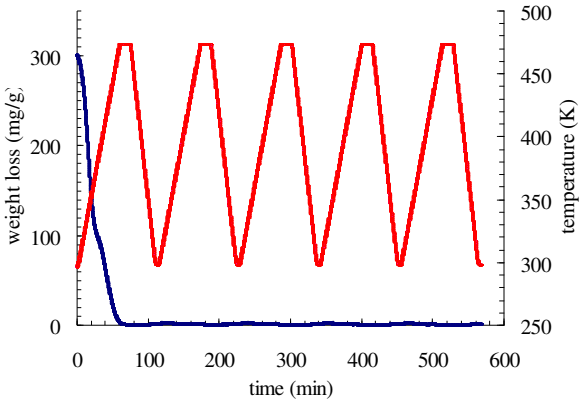

Figure S4. Cycled thermogravimetric analysis.

Figure S5 shows that the N_2 adsorption isotherm at 77 K on the Cu-BTC exhibits two particular regions as already observed by Vishnyakov *et al.*[1], Krungleviciute *et al.*[2] (adsorption of argon at 87 K) and by Krawiec *et al.* (adsorption of N_2 at 77 K).[3]

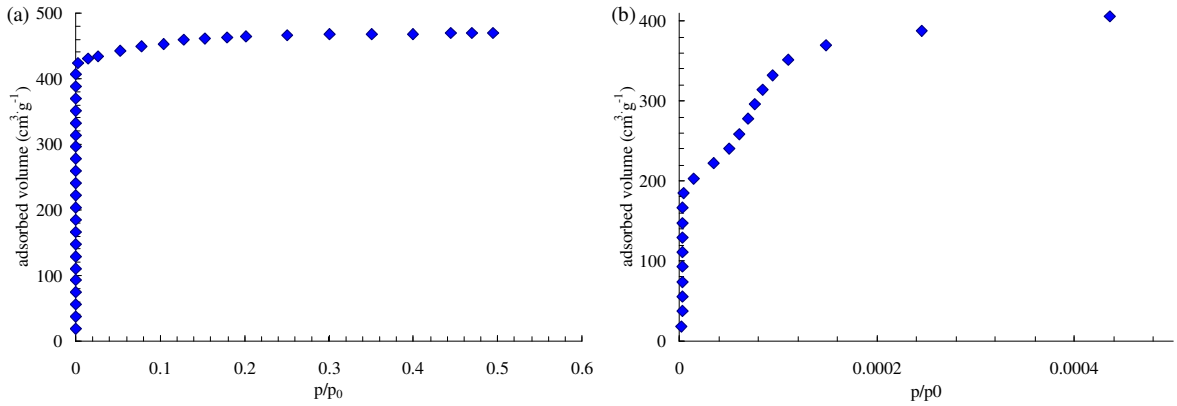

Figure S5. Nitrogen adsorption isotherm at 77 K for pressures up to 0.6 p/p_0 (a) and focused up to 0.0005 p/p_0 (b).

For the lowest pressures (Figure S5b), a first step is observed for pressures between $1 \cdot 10^{-5}$ and $5 \cdot 10^{-5}$ p/p_0. According to previous works,[1-4] this step should correspond to the formation of the first monolayer of adsorbate which fills all the accessible microporous material, *i.e.* adsorption occurs in the octahedral side pockets and in the main channels: calculated BET surface area is of 2211 $m^2 \cdot g^{-1}$. The second step, observed for pressures greater than $1.5 \cdot 10^{-4}$ p/p_0, corresponds to a BET surface area of 1715 $m^2 \cdot g^{-1}$: this step could be attributed to the formation of a second monolayer in the main channel

whereas the side pockets are already filled. To check the relevance of our measurement for the lowest pressures, a simulation using the code developed by Düren *et al.* was performed to estimate the accessible surface area, which is equivalent to the BET surface area.[5] Using the same parameters as Düren *et al.*, we found an accessible surface of 2265 $m^2 \cdot g^{-1}$ (Düren *et al.* found an accessible surface area of 2153 $m^2 \cdot g^{-1}$ for the same material, the difference could be due to the use of different computing systems). The good agreement between theoretical and experimental BET surface areas proves that this material does not contain any impurity, for example free trimesic acid.

Breakthrough curves experiments

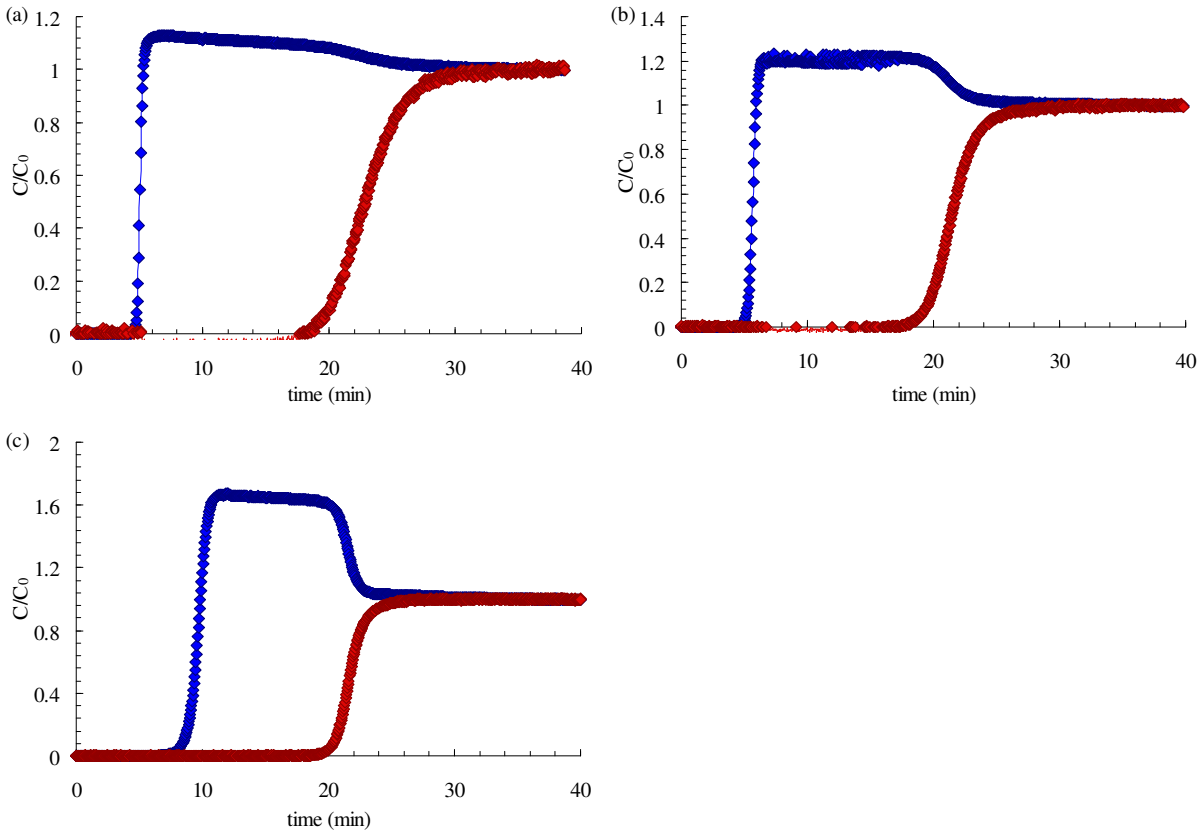

Figure S6. Breakthrough curve of CO_2 (red) and CH_4 (blue) at 0.1 MPa and 303 K for the 25-75 CO_2-CH_4 mixture (a), 50-50 mixture (b) and the 75-25 mixture (c).

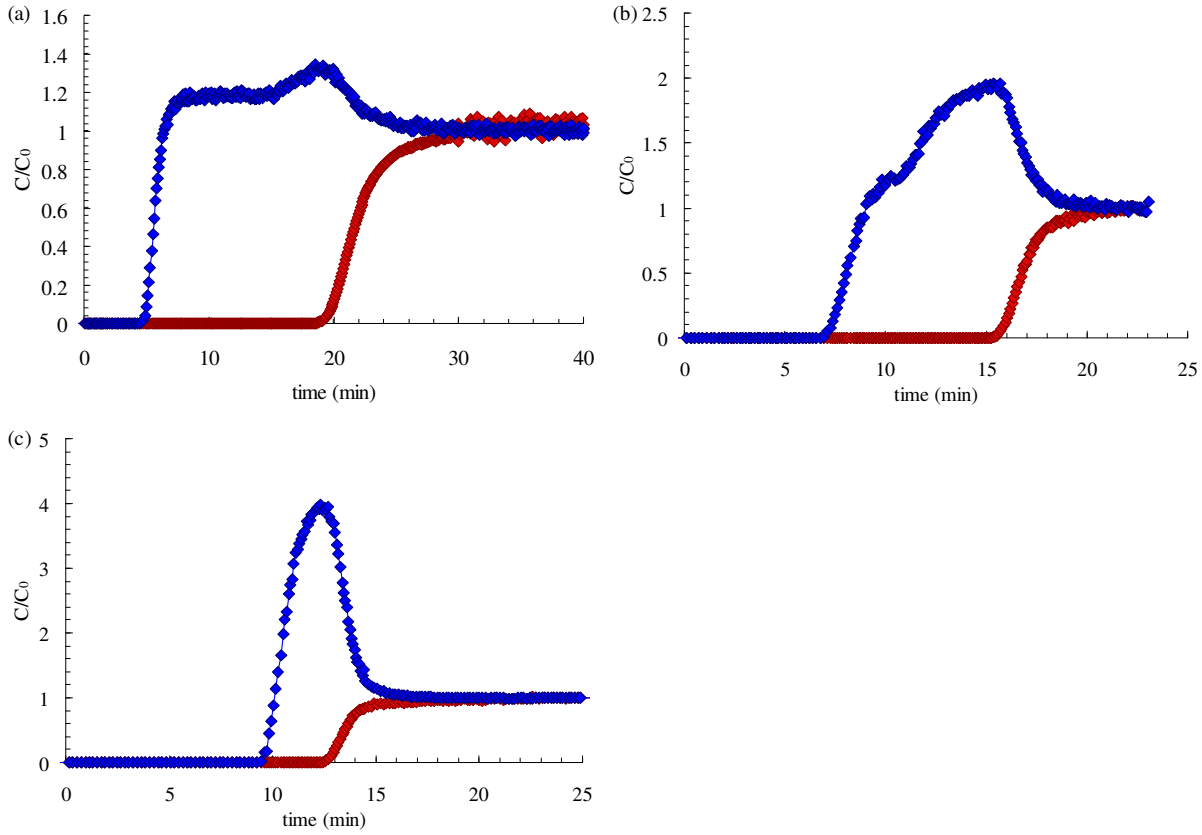

Figure S7. Breakthrough curve of CO_2 (red) and CH_4 (blue) at 1.0 MPa and 303 K for the 25-75 CO_2-CH_4 mixture (a), 50-50 mixture (b) and the 75-25 mixture (c).

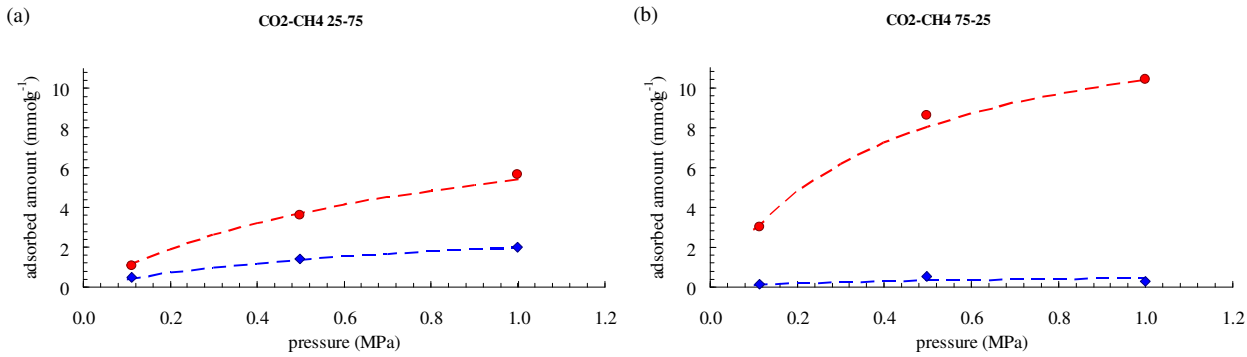

Figure S8. Adsorption isotherms of CO_2 and CH_4 at 303 K (red: CO_2; blue: CH_4; diamonds: breakthrough experimental data; dashed lines: multicomponent Langmuir model based on binary breakthrough experiments; a: 25-75 CO_2-CH_4 mixture; b: 75-25 CO_2-CH_4 mixture).

Breakthrough curves simulations

Table S1. Input parameters of the model.

parameters	values
ε_i	0.403
D_L	$1.0 \cdot 10^{-5}$ m$^2 \cdot$s^{-1}
$D_{C\,CO_2}$	$1 \cdot 10^{-10}$ m$^2 \cdot$s^{-1}
$D_{C\,CH_4}$	$1 \cdot 10^{-10}$ m$^2 \cdot$s^{-1}
R_c	$8.5 \cdot 10^{-6}$ m
k_t	$1 \cdot 10^{-2}$ m$\cdot$s^{-1}
v_0	$9.02 \cdot 10^{-3}$ m$\cdot$s^{-1}
C_{CO_2}	22.14 mol$\cdot$m^{-3}
C_{CH_4}	22.14 mol$\cdot$m^{-3}
column length	0.1 m
column radius	0.035 m
adsorbent mass	2.03 g

Table S2. Isotherm parameters of the model.

	Langmuir based on pure component isotherms	Langmuir based on co-adsorption data
$q_{CO_2,sat}$	13373 mol$\cdot$m^{-3}	13777 mol$\cdot$m^{-3}
$q_{CH_4,sat}$	12307 mol$\cdot$m^{-3}	8950 mol$\cdot$m^{-3}
b_{CO_2}	8.07 m$^3\cdot$mol^{-1}	$7.5 \cdot 10^{-3}$ m$^3\cdot$mol^{-1}
b_{CH_4}	1.30 m$^3\cdot$mol^{-1}	$1.41 \cdot 10^{-3}$ m$^3\cdot$mol^{-1}

References

(1) Vishnyakov, A.; Ravikovitch, P. I.; Neimark, A. V.; Bulow, M.; Wang, Q. M. Nanopore structure and sorption properties of Cu-BTC metal-organic framework. *Nano Lett.* **2003,** *3*, 713.

(2) Krungleviciute, V.; Lask, K.; Heroux, L.; Migone, A. D.; Lee, J. Y.; Li, J.; Skoulidas, A. Argon adsorption on Cu-3(Benzene-1,3,5-tricarboxylate)(2)(H2O)(3) metal-organic framework. *Langmuir* **2007,** *23*, 3106.

(3) Krawiec, P.; Kramer, M.; Sabo, M.; Kunschke, R.; Frode, H.; Kaskel, S. Improved hydrogen storage in the metal-organic framework Cu-3(BTC)(2). *Adv. Eng. Mater.* **2006,** *8*, 293.

(4) Walton, K. S.; Snurr, R. Q. Applicability of the BET method for determining surface areas of microporous metal-organic frameworks. *J. Am. Chem. Soc.* **2007,** *129*, 8552.

(5) Duren, T.; Millange, F.; Ferey, G.; Walton, K. S.; Snurr, R. Q. Calculating geometric surface areas as a characterization tool for metal-organic frameworks. *J. Phys. Chem. C* **2007,** *111*, 15350.